A primer on geodynamics

S. Labrosse

LGL-TPE, Université Claude Bernard Lyon 1, Ens de Lyon, CNRS

Les Houches, July 2021

Outline

Sadi Carnot (1796–1832)

RÉFLEXIONS

SUR LA

PUISSANCE MOTRICE

DU FEU.

Personne n'ignore que la chaleur peut être la cause du mouvement, qu'elle possède même une grande puissance motrice: les machines à vapeur, aujourd'hui si répandues, en sont une preuve parlante à tous les yeux.

C'est à la chaleur que doivent être attribués les grands mouvemens qui frappent nos regards sur la terre; c'est à elle que sont dues les agitations de l'atmosphère, l'ascension des nuages, la chute des pluies et des autres météores, les courans d'eau qui sillonnent la surface du globe et dont l'homme est parvenu à employer pour son usage une faible partie; enfin les tremblemens de terre, les éruptions volcaniques, reconnaissent aussi pour cause la chaleur.

Convection in planetary interiors

- Solid state convection:
  - Solid surface planets and planetary objects (icy satellites, dwarf planets) show signs of deformation in the solid state, whether active or in their past.
  - In many cases: thermal convection.
  - Very large viscosity $\Longrightarrow$ slow motion. The bottleneck for the thermal evolution of planetary objects with solid surface.
  - Convection can also happen in solid shells or spheres deep inside planetary objects: inner core, HP ice layers of Titan, Ganymede.
- Liquid layers:
  - In many cases, a liquid layer exists below: metallic core, water ocean.
  - Early planets most likely start liquid: magma oceans.
  - Dynamics influenced by rotation, magnetic field, imposed externally (magneto-convection) or self-generated (dynamo).

In order to pose a fluid dynamical problem, we write:

- Conservations equations: mass, momentum, energy.
  - Well established, universal although several level of approximations are possible.
- Boundary conditions (BC): classical ones (Dirichlet, Neumann, Robin) or more exotic (phase change BC).
- Constitutive equations: Fourier's law, rheology, equation of state.
  - Can be quite complex.
  - Generally poorly constrained for the Earth interior.

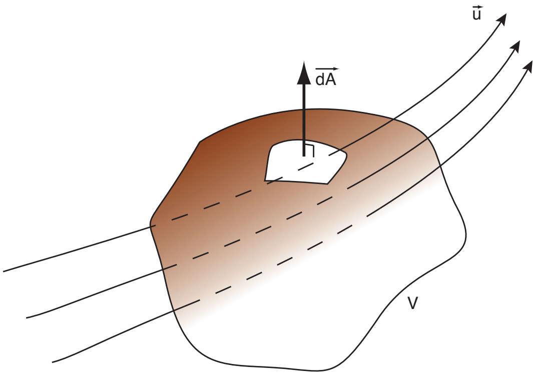

- Consider a fixed control volume.
- The balance equation for a quantity with mass density f is written:

$$\frac{\partial}{\partial t}\int_V \rho f \,\mathrm{d}V = -\int_A \vec{J}_f \cdot \mathrm{d}\vec{A} + \int_V \sigma_f \,\mathrm{d}V$$

where the flux $\vec{J}_f$ and the production σ_f express basic laws of physics.

- Use Gauss' theorem:

$$\Rightarrow \frac{\partial \rho f}{\partial t} = -\vec{\nabla}\cdot\vec{J}_f + \sigma_f$$

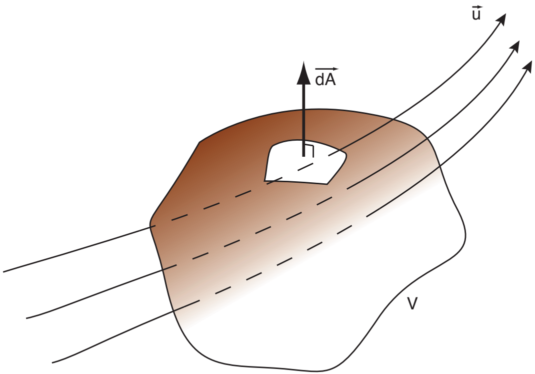

- Consider a fixed control volume.
- The balance equation for a quantity with mass density f is written:

$$\frac{\partial}{\partial t}\int_V \rho f \,\mathrm{d}V = -\int_A \vec{J}_f \cdot \mathrm{d}\vec{A} + \int_V \sigma_f \,\mathrm{d}V$$

where the flux $\vec{J}_f$ and the production σ_f express basic laws of physics.

- Use Gauss' theorem:

$$\Rightarrow \frac{\partial \rho f}{\partial t} = -\vec{\nabla}\cdot\vec{J}_f + \sigma_f$$

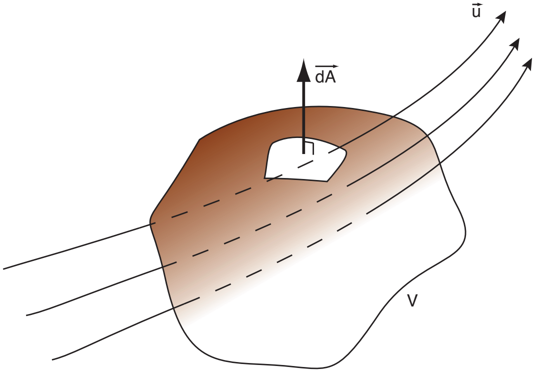

- Consider a fixed control volume.
- The balance equation for a quantity with mass density f is written:

$$\frac{\partial}{\partial t}\int_V \rho f \, \mathrm{d}\, V = -\int_A \vec{J}_f \cdot \mathrm{d}\vec{A} + \int_V \sigma_f \, \mathrm{d}\, V$$

where the flux $\vec{J}_f$ and the production σ_f express basic laws of physics.

- Use Gauss' theorem:

$$\Rightarrow \frac{\partial \rho f}{\partial t} = -\vec{\nabla} \cdot \vec{J}_f + \sigma_f$$

- No production: $\Rightarrow \sigma_f = 0$
- Convective flow only: $\vec{J}_f = \rho \vec{u}$

$$\frac{\partial}{\partial t}\int_V \rho \,\mathsf{d}\,V = -\int_A \rho\vec{u}\cdot \mathsf{d}\vec{A} \Rightarrow \int_V \frac{\partial \rho}{\partial t} = -\int_V \vec{\nabla}\cdot(\rho\vec{u})\,\mathsf{d}\,V$$

$$\Rightarrow \frac{\partial \rho}{\partial t} + \vec{u}\cdot\vec{\nabla}\rho \equiv \frac{\mathsf{D}\rho}{\mathsf{D}t} = \rho\vec{\nabla}\cdot\vec{u}$$

- Incompressible flow: $\vec{\nabla}\cdot\vec{u} = 0$.
- Note

$$\frac{\mathsf{D}}{\mathsf{D}t} \equiv \frac{\partial}{\partial t} + \vec{u}\cdot\vec{\nabla}.$$

$$\rho \frac{D\vec{u}}{Dt} = -\vec{\nabla} P + \vec{\nabla} \cdot \vec{\vec{\tau}} + \rho \vec{g}$$

Local expression of Newton's 2^{nd} law with

- forces applied to the surface: pressure P and deviatoric stress $\vec{\vec{\tau}}$.
- Note: total stress $\vec{\vec{\sigma}} = -P\vec{\vec{I}} + \vec{\vec{\tau}}$
- body forces: gravity $\rho\vec{g}$.

First principle of thermodynamics leads to:

$$\rho \frac{De}{Dt} = -\vec{\nabla} \cdot \vec{q} - P\vec{\nabla} \cdot \vec{u} + \vec{\vec{\tau}} \colon \vec{\nabla}\vec{u} + \rho h$$

Includes

- Viscous dissipation: $\vec{\vec{\tau}} \colon \vec{\nabla}\vec{u}$
- Radiogenic or tidal heat production: ρh

- Internal energy e is developed as function of two state variables s and ρ (add composition if necessary).

$$de = TdS - PdV \rightarrow \frac{De}{Dt} = T\frac{Ds}{Dt} + \frac{P}{\rho^2}\frac{D\rho}{Dt}$$

- Combine the equation for internal energy:

$$\rho T\frac{Ds}{Dt} = -\vec{\nabla}\cdot\vec{q} + \vec{\vec{\tau}}\colon \vec{\nabla}\vec{u} + \rho h$$

- In the generic form of a conservation equation:

$$\rho\frac{Ds}{Dt} = \underbrace{-\vec{\nabla}\cdot\frac{\vec{q}}{T}}_{exchange} + \underbrace{\frac{-1}{T^2}\vec{q}\cdot\vec{\nabla}T + \frac{\vec{\vec{\tau}}\colon \vec{\nabla}\vec{u} + \rho H}{T}}_{production \geq 0}$$

Depending on the choice of state variable, (T, P) or (T, ρ):

$$\rho C_p \frac{DT}{Dt} = -\vec{\nabla} \cdot \vec{q} + \alpha T \frac{DP}{Dt} + \vec{\vec{\tau}} \colon \vec{\nabla}\vec{u} + \rho h$$

$$\rho C_V \frac{DT}{Dt} = -\vec{\nabla} \cdot \vec{q} + \alpha T K_T \vec{\nabla} \cdot \vec{u} + \vec{\vec{\tau}} \colon \vec{\nabla}\vec{u} + \rho h$$

In the case of incompressibility (Boussinesq approximation, see below), the two equations become identical.

Mechanical boundary conditions (BC)

- Solids (ice, rocky mantle) are very viscous compared to liquid or gaseous adjacent layers (ocean, atmosphere, liquid core):
  - No resistance from the boundary: free surface BC applied at the deforming boundaries, $z = h$

$$\vec{u}(h) \cdot \vec{\hat{n}} = 0.$$

$$\vec{\vec{\tau}} \cdot \hat{n} - P\hat{n} = \vec{0}.$$

  - Assuming the boundary is weakly deformed, this BC is approximated by a free–slip BC.

$$u_z(z=0) = 0,$$

$$\tau_{xz}(z=0) = \tau_{yz}(z=0) = \tau_{zz}(z=0) - P(z=0) = 0.$$

- Conversely, liquid layers in contact with solids (i.e. laboratory experiments, the liquid core) obey to a no–slip BC:

$$\vec{u}(z=0) = \vec{0}$$

- Solids in contact with low viscosity fluids above and/or below that can be considered as well mixed: uniform temperature.
- Experiments: fluid in contact with a lid. Continuity of temperature and heat flux. In dimensionless form, it can be shown to be written as a Robin BC:

$$Bi\theta + \frac{\partial \theta}{\partial z} = 0$$

  with θ the temperature anomaly and Bi the Biot number.
  - $Bi \to \infty$: fixed temperature (Dirichlet BC)
  - $Bi \to 0$: fixed flux (Neumann BC)

  Reality is often in–between. May apply to the effect of continents on mantle convection (Grigné et al., 2007a,b) or the upper surface of a magma ocean in contact with an atmosphere (Clarté et al., 2021).

Constitutive equations 1: Fourier's law

$$\vec{q} = -k\vec{\nabla} T$$

- Second principle:

$$\frac{-1}{T^2}\vec{q} \cdot \vec{\nabla} T = k\left(\frac{\vec{\nabla} T}{T}\right)^2 \geq 0 \Rightarrow k > 0$$

- Valid for a very wide range of materials and temperature gradients.
- For crystals, usually anisotropic (see J.-P. Montagner's and A. Tommasi's lectures):

$$\vec{q} = -\vec{\vec{k}} \cdot \vec{\nabla} T \Leftrightarrow q_i = -k_{ij}\partial_j T$$

  This is probably the case in the Earth's mantle where seismic anisotropy is measured.
- Second principle : eigenvalues of $\vec{\vec{k}} > 0$

Constitutive equations 1: Fourier's law

$$\vec{q} = -k\vec{\nabla}T$$

- Second principle:
$$\frac{-1}{T^2}\vec{q}\cdot\vec{\nabla}T = k\left(\frac{\vec{\nabla}T}{T}\right)^2 \geq 0 \Rightarrow k > 0$$
- Valid for a very wide range of materials and temperature gradients.
- For crystals, usually anisotropic (see J.-P. Montagner's and A. Tommasi's lectures):
$$\vec{q} = -\vec{\vec{k}}\cdot\vec{\nabla}T \Leftrightarrow q_i = -k_{ij}\partial_j T$$
This is probably the case in the Earth's mantle where seismic anisotropy is measured.
- Second principle : eigenvalues of $\vec{\vec{k}} > 0$

Constitutive equations 2: Rheology

- Total stress $\vec{\vec{\sigma}}$ has to be related to the strain rate tensor, $\vec{\vec{e}} = \frac{1}{2}(\nabla \vec{u} + \nabla \vec{u}^T) \equiv (\partial_j u_i + \partial_i u_j)/2$, isolating the thermodynamic pressure, P:

$$\vec{\vec{\sigma}} = -P\vec{\vec{I}} + \vec{\vec{F}}(\vec{\vec{e}}).$$

- Newtonian rheology: $\vec{\vec{F}}$ is a linear function. Assuming isotropy and no bulk viscosity (resistance to change of volume) leads to

$$\sigma_{ij} = -P\delta_{ij} + \eta\left(\frac{\partial u_i}{\partial x_j} + \frac{\partial u_j}{\partial x_i} - \frac{2}{3}\delta_{ij}\nabla\cdot\boldsymbol{u}\right).$$

- Second principle of thermodynamics $\Longrightarrow$ viscosity $\eta \geq 0$.

Constitutive equations 2: Rheology

- Total stress $\vec{\vec{\sigma}}$ has to be related to the strain rate tensor, $\vec{\vec{e}} = \frac{1}{2}(\boldsymbol{\nabla}\vec{u} + \boldsymbol{\nabla}\vec{u}^T) \equiv (\partial_j u_i + \partial_i u_j)/2$, isolating the thermodynamic pressure, P:

$$\vec{\vec{\sigma}} = -P\vec{\vec{I}} + \vec{\vec{F}}(\vec{\vec{e}}).$$

- Newtonian rheology: $\vec{\vec{F}}$ is a linear function. Assuming isotropy and no bulk viscosity (resistance to change of volume) leads to

$$\sigma_{ij} = -P\delta_{ij} + \eta\left(\frac{\partial u_i}{\partial x_j} + \frac{\partial u_j}{\partial x_i} - \frac{2}{3}\delta_{ij}\boldsymbol{\nabla}\cdot\boldsymbol{u}\right).$$

- Second principle of thermodynamics $\Longrightarrow$ viscosity $\eta \geq 0$.

Constitutive equations 2: Rheology

- Total stress $\vec{\vec{\sigma}}$ has to be related to the strain rate tensor, $\vec{\vec{e}} = \frac{1}{2}(\boldsymbol{\nabla}\vec{u} + \boldsymbol{\nabla}\vec{u}^T) \equiv (\partial_j u_i + \partial_i u_j)/2$, isolating the thermodynamic pressure, P:

$$\vec{\vec{\sigma}} = -P\vec{\vec{I}} + \vec{\vec{F}}(\vec{\vec{e}}).$$

- Newtonian rheology: $\vec{\vec{F}}$ is a linear function. Assuming isotropy and no bulk viscosity (resistance to change of volume) leads to

$$\sigma_{ij} = -P\delta_{ij} + \eta\left(\frac{\partial u_i}{\partial x_j} + \frac{\partial u_j}{\partial x_i} - \frac{2}{3}\delta_{ij}\boldsymbol{\nabla}\cdot\boldsymbol{u}\right).$$

- Second principle of thermodynamics $\Longrightarrow$ viscosity $\eta \geq 0$.

Constitutive equations 2: Rheology

- Total stress $\vec{\vec{\sigma}}$ has to be related to the strain rate tensor, $\vec{\vec{e}} = \frac{1}{2}(\boldsymbol{\nabla}\vec{u} + \boldsymbol{\nabla}\vec{u}^T) \equiv (\partial_j u_i + \partial_i u_j)/2$, isolating the thermodynamic pressure, P:

$$\vec{\vec{\sigma}} = -P\vec{\vec{I}} + \vec{\vec{F}}(\vec{\vec{e}}).$$

- Newtonian rheology: $\vec{\vec{F}}$ is a linear function. Assuming isotropy and no bulk viscosity (resistance to change of volume) leads to

$$\sigma_{ij} = -P\delta_{ij} + \eta\left(\frac{\partial u_i}{\partial x_j} + \frac{\partial u_j}{\partial x_i} - \frac{2}{3}\delta_{ij}\boldsymbol{\nabla}\cdot\boldsymbol{u}\right).$$

- Second principle of thermodynamics $\Longrightarrow$ viscosity $\eta \geq 0$.

More on this topic to come later and in Fanny Garel's and Andréa Tommasi's lectures.

- Origin of motion: change of density (ρ) with temperature (T).

$\Rightarrow$ Thermal expansion coefficient:

$$\alpha = -\frac{1}{\rho}\left(\frac{\partial \rho}{\partial T}\right)_P$$

- Minimal (linear) equation:

$$\rho = \rho_0 \left[1 - \alpha\,(T - T_0)\right]$$

- Effect of pressure

$$\rho = \rho_0 \left[1 - \alpha\,(T - T_0) + \frac{P - P_0}{K_T}\right]$$

Important but not leading order since pressure variation is dominated by the hydrostatic, i.e. in the direction of $\vec{g}$. Not considered at first!

- Effect of composition: needs additional parameters such as the FeO mass fraction for the Earth mantle. If it is considered, an additional balance equation is needed to compute its evolution.

- Origin of motion: change of density (ρ) with temperature (T).

$\Rightarrow$ Thermal expansion coefficient:

$$\alpha = -\frac{1}{\rho}\left(\frac{\partial \rho}{\partial T}\right)_P$$

- Minimal (linear) equation:

$$\rho = \rho_0 \left[1 - \alpha\,(T - T_0)\right]$$

- Effect of pressure

$$\rho = \rho_0 \left[1 - \alpha\,(T - T_0) + \frac{P - P_0}{K_T}\right]$$

  Important but not leading order since pressure variation is dominated by the hydrostatic, i.e. in the direction of $\vec{g}$. Not considered at first!

- Effect of composition: needs additional parameters such as the FeO mass fraction for the Earth mantle. If it is considered, an additional balance equation is needed to compute its evolution.

- Origin of motion: change of density (ρ) with temperature (T).

$\Rightarrow$ Thermal expansion coefficient:

$$\alpha = -\frac{1}{\rho}\left(\frac{\partial \rho}{\partial T}\right)_P$$

- Minimal (linear) equation:

$$\rho = \rho_0 \left[1 - \alpha\left(T - T_0\right)\right]$$

- Effect of pressure

$$\rho = \rho_0 \left[1 - \alpha\left(T - T_0\right) + \frac{P - P_0}{K_T}\right]$$

Important but not leading order since pressure variation is dominated by the hydrostatic, i.e. in the direction of $\vec{g}$. Not considered at first!

- Effect of composition: needs additional parameters such as the FeO mass fraction for the Earth mantle. If it is considered, an additional balance equation is needed to compute its evolution.

- Origin of motion: change of density (ρ) with temperature (T).

$\Rightarrow$ Thermal expansion coefficient:

$$\alpha = -\frac{1}{\rho}\left(\frac{\partial \rho}{\partial T}\right)_P$$

- Minimal (linear) equation:

$$\rho = \rho_0 \left[1 - \alpha\left(T - T_0\right)\right]$$

- Effect of pressure

$$\rho = \rho_0 \left[1 - \alpha\left(T - T_0\right) + \frac{P - P_0}{K_T}\right]$$

  Important but not leading order since pressure variation is dominated by the hydrostatic, i.e. in the direction of $\vec{g}$. Not considered at first!

- Effect of composition: needs additional parameters such as the FeO mass fraction for the Earth mantle. If it is considered, an additional balance equation is needed to compute its evolution.

The Oberbeck–Boussinesq approximation

- Boussinesq (1903) and Oberbeck (1879) propose to simplify the full equations by setting the density constant in all terms but the buoyancy term.
- At the same level of approximation the dissipation is negligible and $C_p = C_v \equiv C$.
- The minimal set of equations for convection are (neglecting internal heating for now)

$$\vec{\nabla} \cdot \vec{u} = 0 \tag{1}$$

$$\rho_0 \left(\frac{\partial \vec{u}}{\partial t} + \vec{u} \cdot \vec{\nabla} \vec{u} \right) = -\vec{\nabla} P + \rho \vec{g} + \eta \vec{\nabla}^2 \vec{u} \tag{2}$$

$$\frac{\partial T}{\partial t} + \vec{u} \cdot \vec{\nabla} T = \kappa \vec{\nabla}^2 T \tag{3}$$

$$\rho = \rho_0 \left[1 - \alpha (T - T_0) \right] \tag{4}$$

- And boundary conditions.

Outline

Introduction

balance equations and the Boussinesq approximation

Rayleigh-Bénard convection

- Historical background
- Linear stability analysis
- Behaviour beyond the onset
- High Rayleigh number dynamics and scaling of heat transfer

Convection in Earth's mantle

- Evidences for mantle convection on Earth
- Internally heated Rayleigh–Bénard convection
- Temperature–dependence of viscosity and more complex rheologies
- Compressibility effects
- Variations of composition
  - Models for the present state
  - Evolution models
- Crust recycling
- Evolution from a primordial layering

Outline

Experiments by Bénard

Bénard (1900a,b, 1901) conducted the first systematic experiments on flow driven by a destabilising temperature difference.

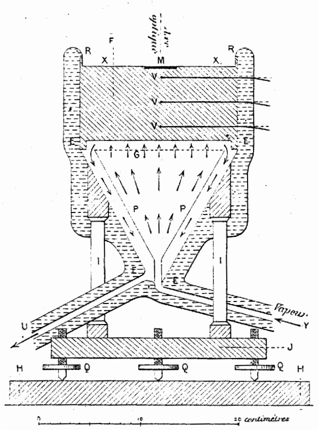

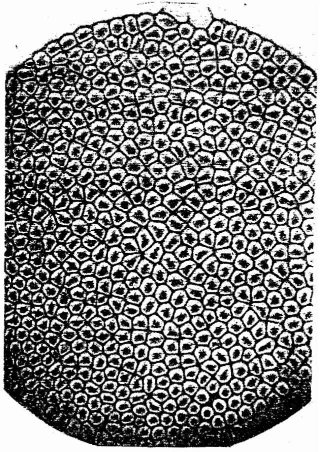

- Organisation of the flow in nearly perfect hexagonal cells (analogy to plant cells).

- Rayleigh (1916) proposed the first theory for the linear stability of a steady conductive state in a gravity field. He showed that a minimum temperature gradient is necessary for the onset of convection, that depends on several physical parameters.
- Block (1956) showed that the flow in Bénard's experiments is not driven by gravity but by temperature–dependence of surface tension, the Marangoni effect. Pearson (1958) developed the corresponding theory.
- Term "Rayleigh–Bénard convection" is still used to denote convection driven by the temperature–dependence of density in a gravity field while Bénard's setup is called Bénard–Marangoni.

(Bénard, 1901)
Topography exaggerated 100x

Fig. 15.

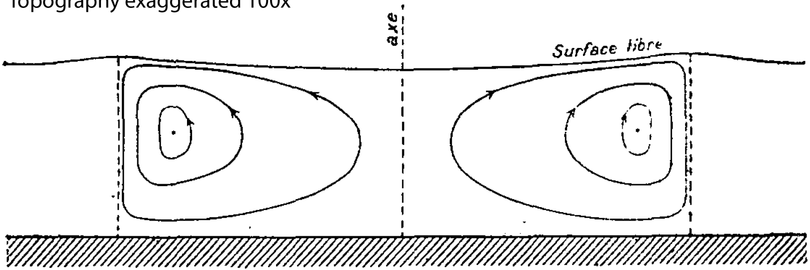

Approaches for thermal convection

The problem is described by a set of coupled non-linear partial differential equations. Several approaches are possible:

- Linearised equations: Linear stability.
- Weakly non-linear theory: valid only very close to the onset of convection.
- Numerical models.
- Experiments.

Numerical models and experiments allow to study various complexities relevant to planetary interiors.

Outline

- The problem (the equations) always admit several solutions, notably a motionless steady conduction solution

$\Rightarrow$ What controls the onset of motion? The (in–)stability of the steady conduction solution.

- What forms do the solutions take with motion?

Dimensional analysis: the Rayleigh number

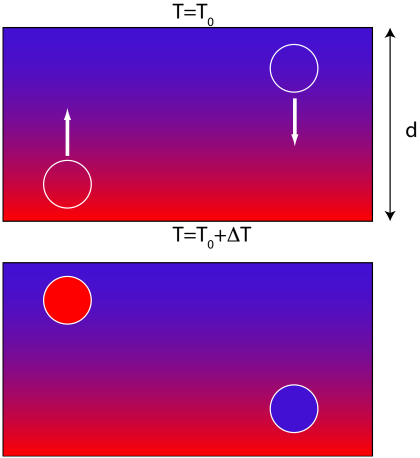

- Buoyancy: $\rho g \alpha \Delta T \sim \rho v/\tau_c \sim \rho d/\tau_c^2$.

$\Rightarrow$ Convective time: $\tau_c^2 = d/g\alpha\Delta T$.

- Diffusive time: $\tau_d = d^2/\kappa$.
- Viscous time: $\tau_v = d^2/\nu = \rho d^2/\eta$
- Convection if $\tau_v \tau_d/\tau_c^2 >> 1$

$$Ra \equiv \frac{\alpha \Delta T g d^3}{\kappa \nu} > R_c \sim 10^3$$

Gross estimate for Earth's mantle: $Ra \sim 10^8$

Dimensional analysis: the Rayleigh number

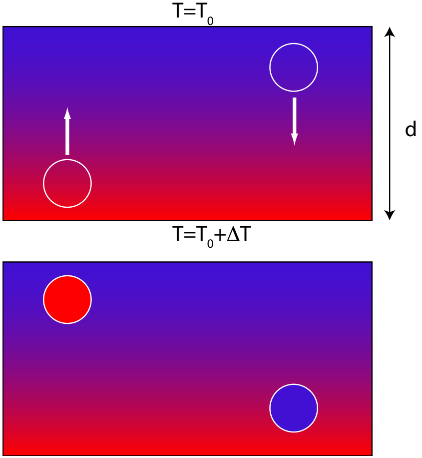

- Buoyancy: $\rho g \alpha \Delta T \sim \rho v/\tau_c \sim \rho d/\tau_c^2$.

$\Rightarrow$ Convective time: $\tau_c^2 = d/g\alpha\Delta T$.

- Diffusive time: $\tau_d = d^2/\kappa$.
- Viscous time: $\tau_v = d^2/\nu = \rho d^2/\eta$
- Convection if $\tau_v \tau_d/\tau_c^2 >> 1$

$$Ra \equiv \frac{\alpha \Delta T g d^3}{\kappa \nu} > R_c \sim 10^3$$

Gross estimate for Earth's mantle: $Ra \sim 10^8$

Dimensional analysis: the Rayleigh number

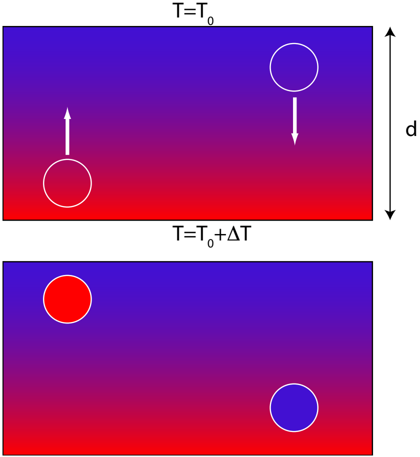

- Buoyancy: $\rho g \alpha \Delta T \sim \rho v/\tau_c \sim \rho d/\tau_c^2$.

$\Rightarrow$ Convective time: $\tau_c^2 = d/g\alpha\Delta T$.

- Diffusive time: $\tau_d = d^2/\kappa$.
- Viscous time: $\tau_v = d^2/\nu = \rho d^2/\eta$
- Convection if $\tau_v \tau_d/\tau_c^2 >> 1$

$$Ra \equiv \frac{\alpha \Delta T g d^3}{\kappa \nu} > R_c \sim 10^3$$

Gross estimate for Earth's mantle: $Ra \sim 10^8$

Dimensional analysis: the Rayleigh number

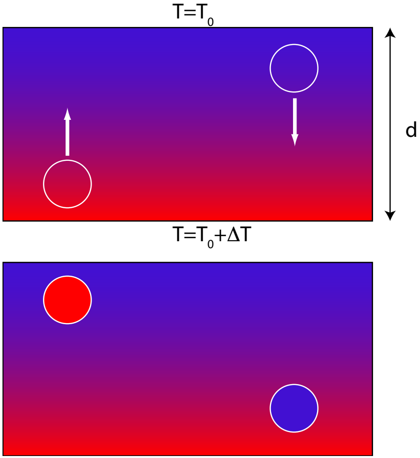

- Buoyancy: $\rho g \alpha \Delta T \sim \rho v / \tau_c \sim \rho d / \tau_c^2$.

$\Rightarrow$ Convective time: $\tau_c^2 = d / g \alpha \Delta T$.

- Diffusive time: $\tau_d = d^2 / \kappa$.
- Viscous time: $\tau_v = d^2 / \nu = \rho d^2 / \eta$
- Convection if $\tau_v \tau_d / \tau_c^2 >> 1$

$$Ra \equiv \frac{\alpha \Delta T g d^3}{\kappa \nu} > R_c \sim 10^3$$

Gross estimate for Earth's mantle: $Ra \sim 10^8$

Perturbation equations

The system of equation admits a motionless ($\vec{u} = 0$) steady ($\partial_t = 0$) conduction solution:

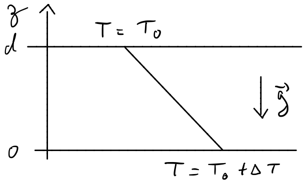

$$\vec{\nabla} P = \rho \vec{g} \tag{5}$$

$$\vec{\nabla}^2 T = 0 \tag{6}$$

$$\rho = \rho_0 \left[1 - \alpha(T - T_0)\right] \tag{7}$$

$$T(d) = T_0 \text{ and } T(0) = T_0 + \Delta T \tag{8}$$

$$\Rightarrow T_c = T_0 + \Delta T - \frac{z}{d} \Delta T \tag{9}$$

$$\rho_c = \rho_0 \left[1 - \alpha \Delta T \left(1 - \frac{z}{d}\right)\right] \Rightarrow P_c = \ldots \tag{10}$$

Write equations for the perturbations of the steady conduction solution, $\theta = T - T_c$, $p = P - P_c$:

$$\vec{\nabla} \cdot \vec{u} = 0 \tag{11}$$

$$\rho_0 \left(\frac{\partial \vec{u}}{\partial t} + \vec{u} \cdot \vec{\nabla} \vec{u}\right) = -\vec{\nabla} p - \rho_0 \alpha \theta \vec{g} + \eta \vec{\nabla}^2 \vec{u} \tag{12}$$

$$\frac{\partial \theta}{\partial t} + \vec{u} \cdot \vec{\nabla} \theta = \frac{\Delta T}{d} u_z + \kappa \vec{\nabla}^2 \theta \tag{13}$$

- There are several ways of doing it but I choose here

$$x', y' = \frac{x, y}{d};\ z' = \frac{z}{d} + \frac{1}{2};\ \theta' = \frac{\theta}{\Delta T};\ t' = \frac{\kappa t}{d^2};\ p' = \frac{pd^2}{\kappa\eta}$$

- We get, after dropping the $'$s:

$$\vec{\nabla} \cdot \vec{u} = 0 \tag{14}$$

$$\frac{1}{Pr}\left(\frac{\partial \vec{u}}{\partial t} + \vec{u} \cdot \vec{\nabla}\vec{u}\right) = -\vec{\nabla}p + \vec{\nabla}^2\vec{u} + Ra\theta\hat{z} \tag{15}$$

$$\frac{\partial \theta}{\partial t} + \vec{u} \cdot \vec{\nabla}\theta = u_z + \vec{\nabla}^2\theta \tag{16}$$

- with

$$Ra = \frac{\rho_0 g \alpha \Delta T d^3}{\kappa\eta} \text{ the Rayleigh number} \tag{17}$$

$$Pr = \frac{\eta}{\rho_0 \kappa} \text{ the Prandtl number} \tag{18}$$

- and boundary conditions at $z = \pm 1/2$

$$\theta = 0;\ u_z = 0;\ \partial_z u_x = \partial_z u_y = 0 \Rightarrow \partial_z^2 u_z = 0.$$

- There are several ways of doing it but I choose here

$$x', y' = \frac{x, y}{d};\; z' = \frac{z}{d} + \frac{1}{2};\; \theta' = \frac{\theta}{\Delta T};\; t' = \frac{\kappa t}{d^2};\; p' = \frac{pd^2}{\kappa\eta}$$

- We get, after dropping the $'$s:

$$\vec{\nabla} \cdot \vec{u} = 0 \tag{14}$$

$$\frac{1}{Pr}\left(\frac{\partial \vec{u}}{\partial t} + \vec{u} \cdot \vec{\nabla}\vec{u}\right) = -\vec{\nabla}p + \vec{\nabla}^2\vec{u} + Ra\theta\hat{z} \tag{15}$$

$$\frac{\partial \theta}{\partial t} + \vec{u} \cdot \vec{\nabla}\theta = u_z + \vec{\nabla}^2\theta \tag{16}$$

- with

$$Ra = \frac{\rho_0 g \alpha \Delta T d^3}{\kappa\eta} \text{ the Rayleigh number} \tag{17}$$

$$Pr = \frac{\eta}{\rho_0 \kappa} \text{ the Prandtl number} \tag{18}$$

- and boundary conditions at $z = \pm 1/2$

$$\theta = 0;\; u_z = 0;\; \partial_z u_x = \partial_z u_y = 0 \Rightarrow \partial_z^2 u_z = 0.$$

- There are several ways of doing it but I choose here

$$x', y' = \frac{x, y}{d}; \; z' = \frac{z}{d} + \frac{1}{2}; \; \theta' = \frac{\theta}{\Delta T}; \; t' = \frac{\kappa t}{d^2}; \; p' = \frac{pd^2}{\kappa\eta}$$

- We get, after dropping the $'$s:

$$\vec{\nabla} \cdot \vec{u} = 0 \tag{14}$$

$$\frac{1}{Pr}\left(\frac{\partial \vec{u}}{\partial t} + \vec{u} \cdot \vec{\nabla}\vec{u}\right) = -\vec{\nabla}p + \vec{\nabla}^2\vec{u} + Ra\theta\hat{z} \tag{15}$$

$$\frac{\partial \theta}{\partial t} + \vec{u} \cdot \vec{\nabla}\theta = u_z + \vec{\nabla}^2\theta \tag{16}$$

- with

$$Ra = \frac{\rho_0 g \alpha \Delta T d^3}{\kappa\eta} \text{ the Rayleigh number} \tag{17}$$

$$Pr = \frac{\eta}{\rho_0 \kappa} \text{ the Prandtl number} \tag{18}$$

- and boundary conditions at $z = \pm 1/2$

$$\theta = 0; \; u_z = 0; \; \partial_z u_x = \partial_z u_y = 0 \Rightarrow \partial_z^2 u_z = 0.$$

The Prandtl number

$$Pr = \frac{\eta}{\rho_0 \kappa}$$

- Characteristics of the working fluid
- Liquid water: $Pr \sim 7$
- Earth's mantle: $Pr \sim 10^{25}$
- Water ice: $Pr \sim 10^{17}$

$\Rightarrow$ Inertia term negligible for convection in solids!

- Kinetic energy of Earth's mantle (mass 1×10^{24} kg), assuming a mean velocity of 3 cm/yr is $\sim 2 \times 10^6$ J. Similar to a car driving at 100 km/hr.

$\Rightarrow$ The Prandtl number is taken as infinite in solids.

Mode decomposition for the linear problem

- Considering infinitely small perturbations of the conduction solution, the problem can be linearised:

$$\vec{\nabla} \cdot \vec{u} = 0 \tag{19}$$

$$\frac{1}{Pr} \frac{\partial \vec{u}}{\partial t} = -\vec{\nabla} p + \vec{\nabla}^2 \vec{u} + Ra\theta\hat{z} \tag{20}$$

$$\frac{\partial \theta}{\partial t} = u_z + \vec{\nabla}^2 \theta \tag{21}$$

- The perturbation can be developed in time–dependent Fourier modes and, for a linear problem, each mode can be analysed independently. The problem is independent of the horizontal orientation and we choose:

$$(\theta, p, u_x, u_z) = (\Theta(z), P(z), U(z), W(z))\mathrm{e}^{\sigma t}\mathrm{e}^{\mathrm{i}kx}.$$

- If $\Re(\sigma) > 0$ the instability grows.
- The conduction solution is stable if *all* modes of perturbation have $\Re(\sigma) < 0$

Solution for free–slip BCs

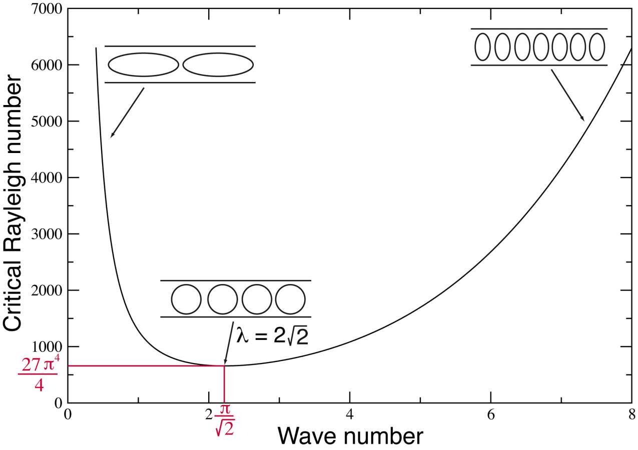

- When both boundaries are free–slip, $W = \cos(\pi z)$ provides the solution.
- Neutral stability:

$$Ra_c = \frac{\left(\pi^2 + k^2\right)^3}{k^2}$$

- Minimum value

$$R_c = \frac{27\pi^4}{4} \simeq 657 \text{ for } k_c = \frac{\pi}{\sqrt{2}}$$

- First unstable mode has wavelength

$$\lambda_c = \frac{2\pi}{k_c} = 2\sqrt{2}.$$

$\Rightarrow$ rolls $\sqrt{2}$ wider than they are tall.

Effect of mechanical BCs on the linear stability

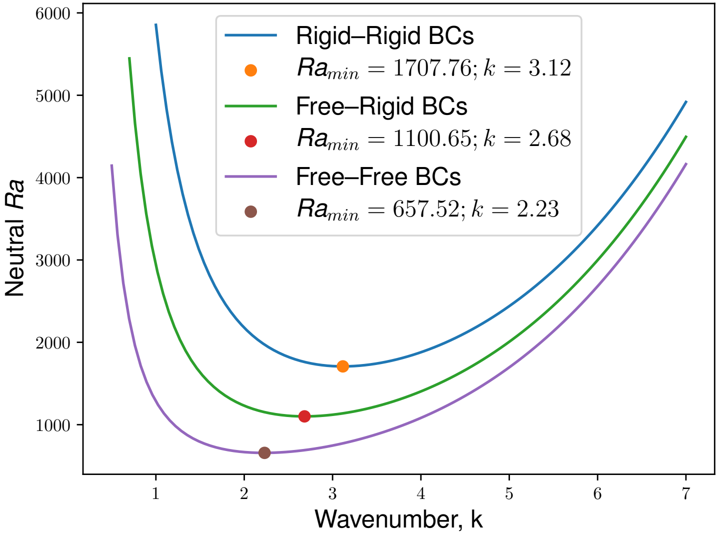

Outline

Example calculation close to onset

- $Ra = 800, \; Pr = \infty$.
- Aspect ratio $= 32 \times 32 \times 1$.
- Initial condition: conductive solution plus random noise.
- Pattern dynamics with long–distance interactions between defects.
- Steady–state: Rolls at $\pi/4$ angle so that a natural number of $2\sqrt{2}$ wavelength fit.

Stability of finite amplitude solutions

- Schlüter et al. (1965) showed that only rolls are stable finite solution close to the onset of convection.
- Busse (1967) showed that a finite range of wavenumber leads to stable roll solution.

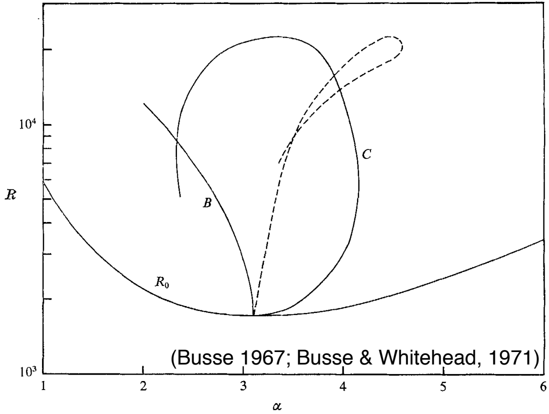

FIGURE 1. Stability region of convection rolls. The zigzag instability and the cross-roll instability produce the stability boundaries B and C, respectively. The dashed line denotes the value of the wave-number $\tilde{\alpha}$ of the marginal cross-roll disturbances along curve C.

- Many experiments (starting with Bénard's) lead to hexagonal patterns.
- Hexagonal patterns are non–symmetrical with respect to $z \to -z$ tranformation, whereas rolls are.
- Hexagonal flow is obtained for asymmetrical conditions such as provided by depth– or temperature–dependent properties (e.g. $\eta(T)$) or volumetric heat generation.

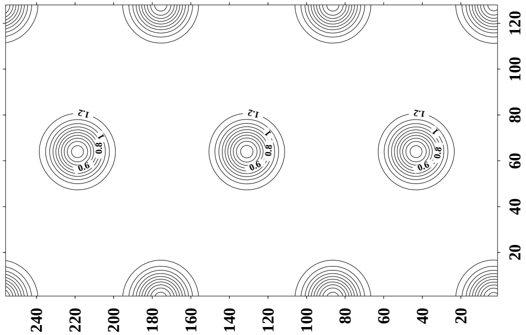

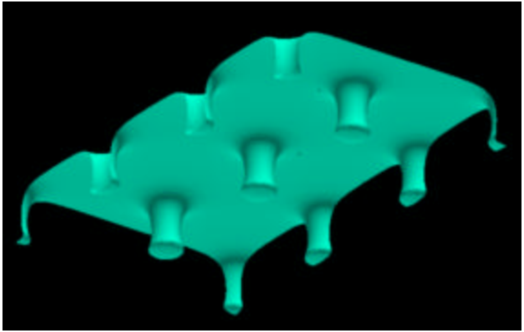

Outline

Example calculation at high *Ra*

- *Ra* $= 10^7$, *Pr* $= \infty$, aspect ratio $4 \times 4 \times 1$
- Initial conditions: $T = 1/2$ and exponential variation in thin layers to match BCs plus small random noise.
- Two iso-temperature surface represented.

Regime diagram in the (Ra, Pr) space

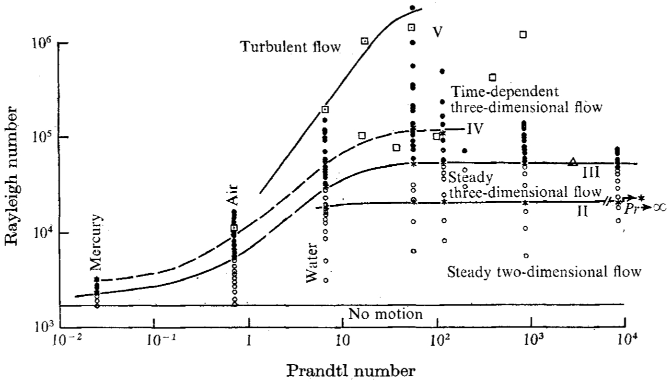

FIGURE 4. Regime diagram. ○, steady flows; ●, time-dependent flows; ★, transition points with observed change in slope; □, Rossby's observations of time-dependent flow; ⊡, Willis & Deardorff's (1967*a*) observations for turbulent flow; △, Silveston's point of transition for time-dependent flow (see text).

(Krishnamurti, 1973)

$Ra = 10^7$

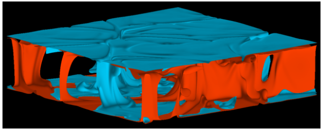

$Ra = 10^5$

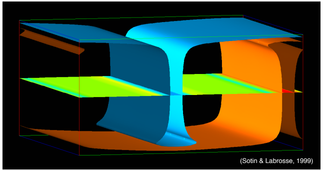

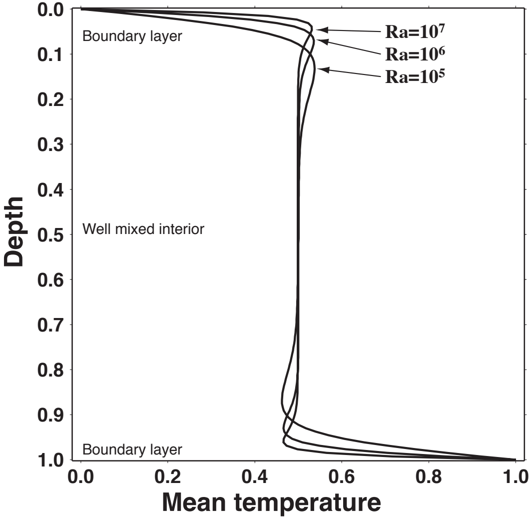

- Efficient mixing in the bulk of the domain $\Rightarrow$ uniform temperature.
- Matching the boundary conditions $\Rightarrow$ boundary layers.
- Increasing the Rayleigh number makes the thickness of boundary layers decrease.

Simple dimensional argument for the heat flow

- Dimensionless heat flow $Nu = qd/k\Delta T = f(Ra) = ARa^{\beta}$ to be valid over large range of Ra values.
- At very large Ra, boundary layers and the resulting plumes get very small.
- The dynamics of convection and the resulting heat flow should become independent of the total thickness:
$$q = A\frac{k\Delta T}{d}\left(\frac{g\alpha\Delta T d^3}{\kappa\nu}\right)^{\beta} \Rightarrow \beta = \frac{1}{3}.$$
- More on that during Maylis Landeau's practical.

Experiments at very high *Ra*
Niemela et al. (2000)

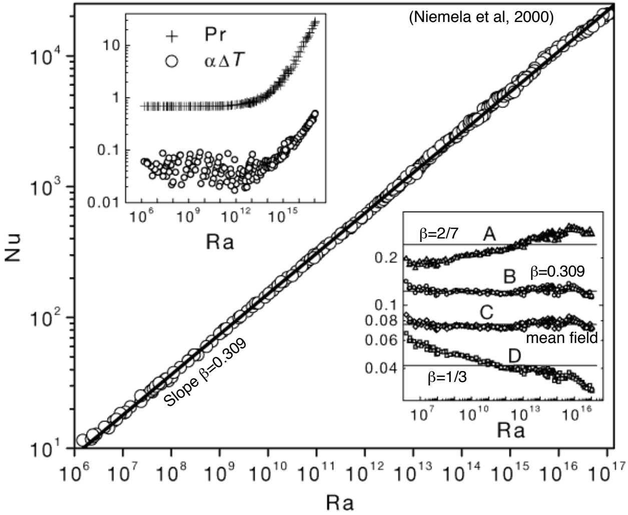

- Working fluid: cryogenic helium.
- *Pr* ~ 1
- 1 m–high tank.
- Exponent β close to but different from $1/3$.

Outline

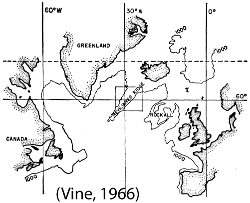
60°W
30°W
0°
GREENLAND
REYKJANES RIDGE
ROCKALL
CANADA
1000
60°

(Vine, 1966)

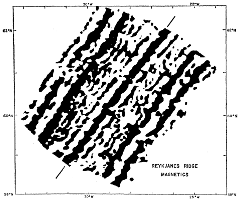
REYKJANES RIDGE
MAGNETICS

Plate tectonics

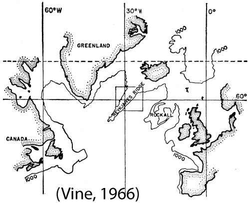

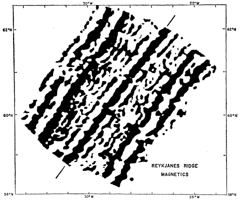

(Vine, 1966)

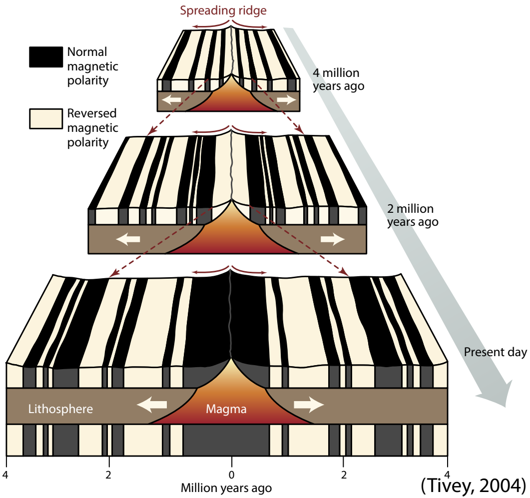

(Tivey, 2004)

Plate tectonics

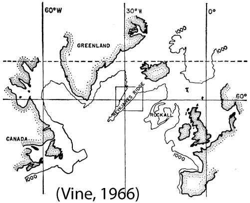

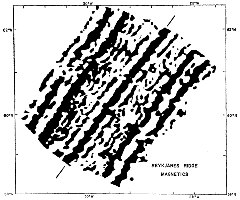

(Vine, 1966)

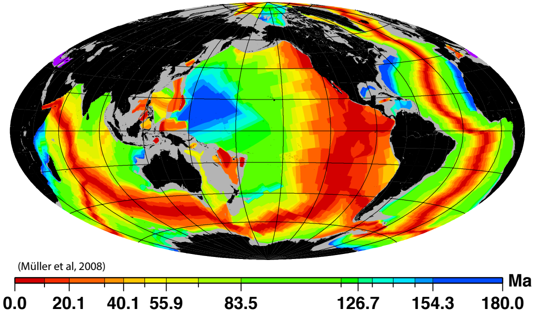

(Müller et al, 2008)

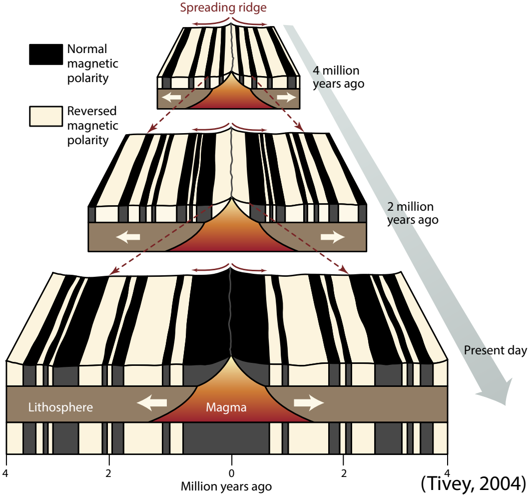

(Tivey, 2004)

Thermal structure of the oceanic lithosphere

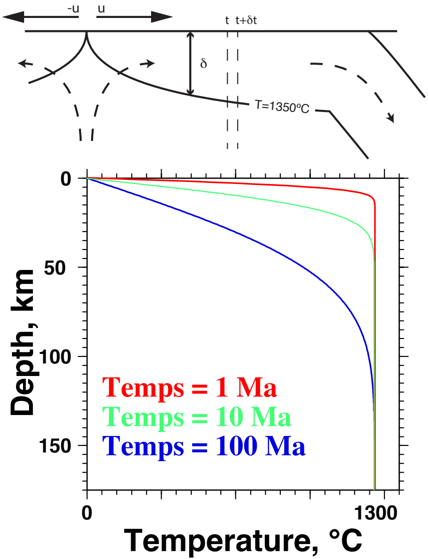

- A cold front propagates downward in the mantle as the plate moves away from the ridge
- The temperature follows the solution for the cooling of an infinite half–space:

$$T(z) = T_M \operatorname{erf} \frac{z}{2\sqrt{\kappa t}}$$
$$= \frac{2\,T_M}{\sqrt{\pi}} \int_0^{z/2\sqrt{\kappa t}} e^{-x^2}\,dx$$

- The heat flux decrease with the age of the plate as

$$q(t) = \frac{kT_M}{\sqrt{\pi \kappa t}} = C_Q t^{-1/2}$$

- C_Q can be determined by fitting the observed flux in well sedimented areas.

Heat flow data from well–sedimented areas

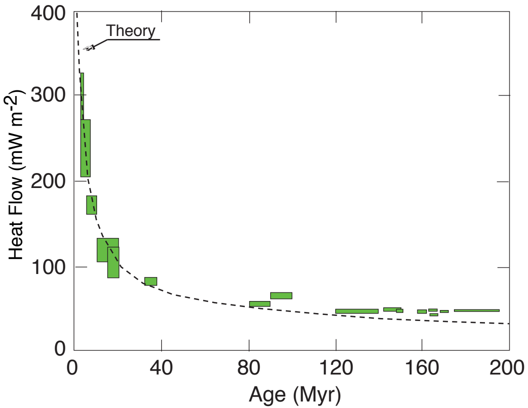

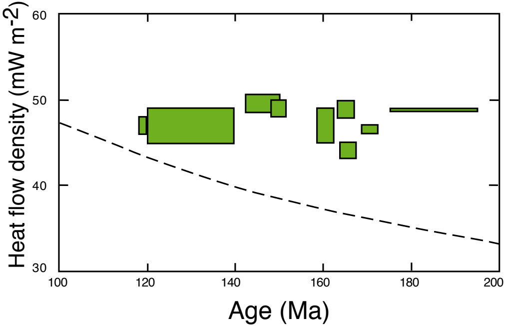

(Lister et al., 1990)

- $q = C_Q/\sqrt{t}$ valid for t up to 80 Myr with $475 \leq C_Q \leq 500 \Rightarrow T_M = 1300\,^{\circ}$C.
- Deviations for ages > 80 Myr: small–scale convection under the lithosphere.

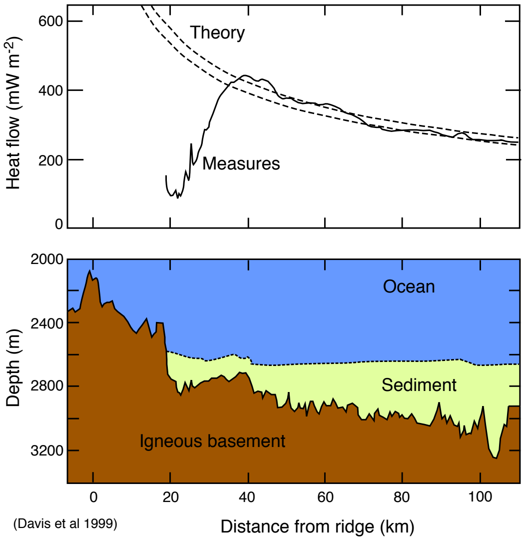

(Davis et al 1999)

- Impressive match between theory and observations when the sedimentary cover is sufficient
  - to properly measure the heat flow
  - and limit hydrothermal activity.

Another piece of evidence: Topography

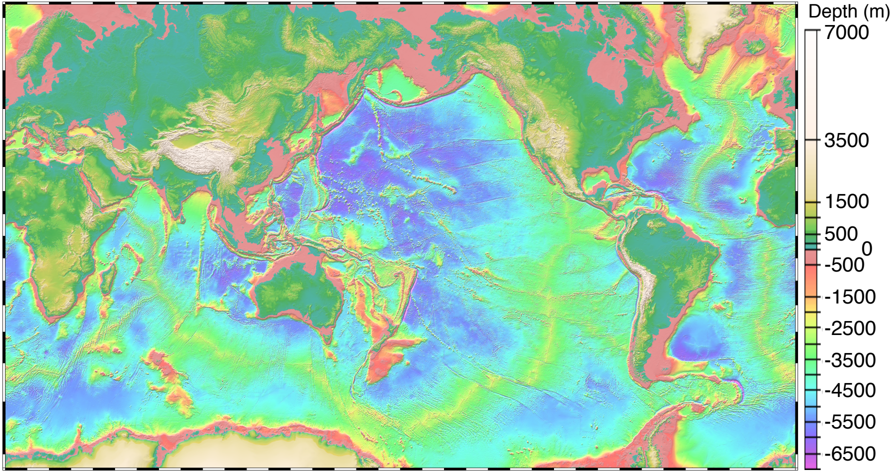

(Smith and Sandwell, 1997)

Isostatic theory for the ocean topography

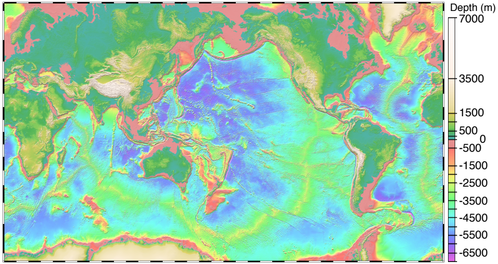

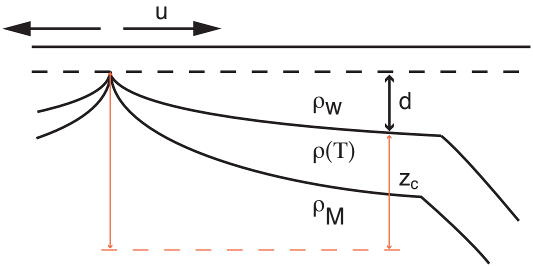

Thermal contraction ⇒ subsidence of the seafloor with age.

$$z = \frac{\rho_M}{\rho_M - \rho_w} 2\alpha T_M \sqrt{\frac{\kappa t}{\pi}}$$

Test of the theory

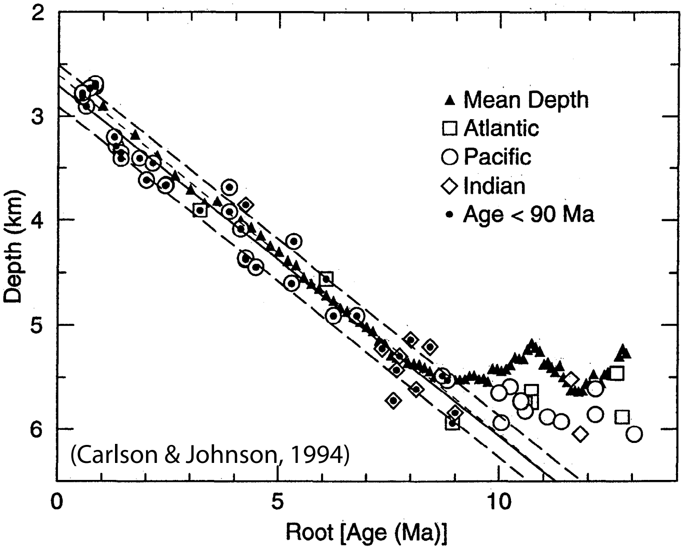

Oceanic heat flow

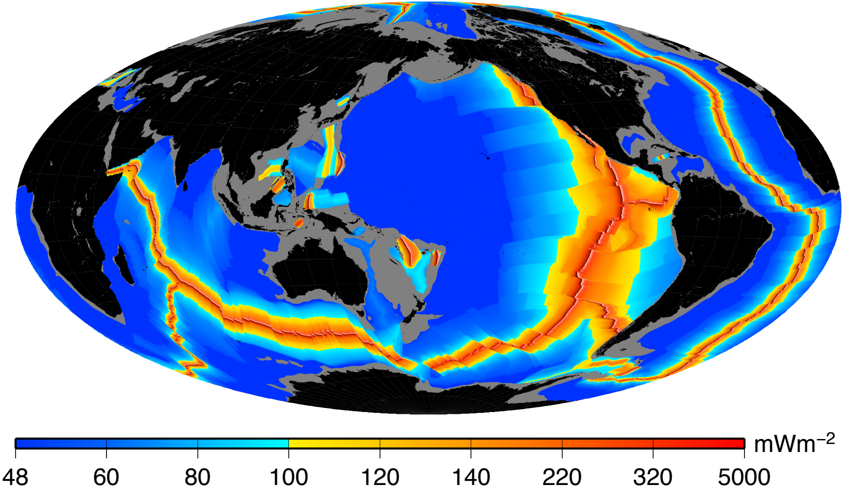

- Total: 29 ± 1 TW from normal oceans.
- Add 2 TW to 4 TW from hotspots.

Total heat flow at Earth's surface
Jaupart et al. (2015)

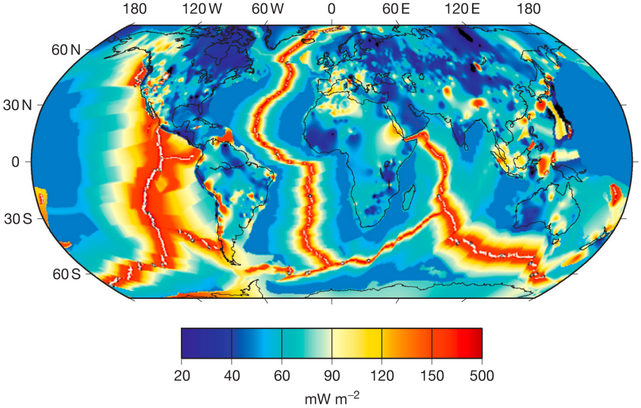

- The total heat loss of the Earth is $\simeq$ 46 TW
- The average heat flow density is 90 mW m^{-2}, corresponding to a mean temperature gradient of 30 K km^{-1}. The gradient must level off to match a central temperature $T_c \sim$ 6000 K.

$\Rightarrow$ A more efficient heat transfer mechanism is necessary at depth.

Advection in the mantle: order of magnitude

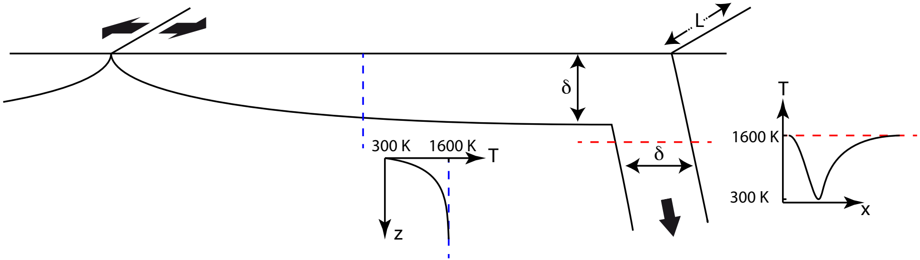

- Subduction :
  - length $L = 48\,800$ km.
  - mean temperature anomaly $\delta T \sim 600$ K.
  - typical velocity $w \sim 10$ cm/yr
  - thickness $\delta x \sim 100$ km

  $\Rightarrow$ Total advective flux: $Q = \delta x L \rho C_p w \delta T \simeq 30$ TW
- Plumes: very small surface $\Rightarrow$ 2 TW

Computation of the predicted temperature variations induced in the mantle by injection of cold plates in the past ~ 180 Ma (Ricard et al., 1993) and comparison with tomographic models.

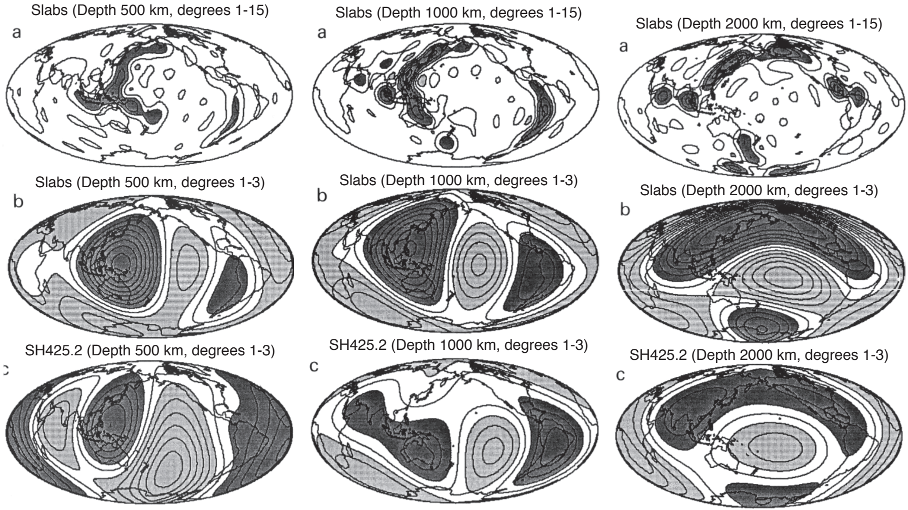

(Ricard et al, 1993) (Ricard et al, 1993) (Ricard et al, 1993)

Computation of the predicted temperature variations induced in the mantle by injection of cold plates in the past ~ 180 Ma (Ricard et al., 1993) and comparison with tomographic models.

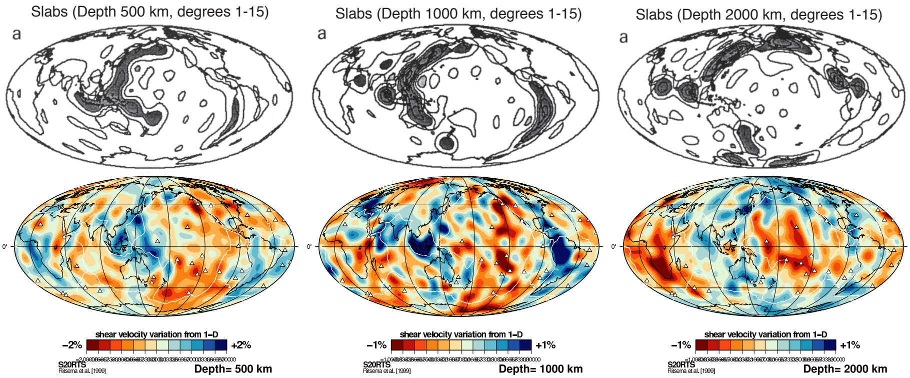

Seismic tomography: Ritsema et al. (1999).

Some peculiarities of mantle convection

- Internally heated by radioactivity and secularly cooled.
- Spherical shell geometry.
- Temperature–dependent viscosity and even complex rheology. Necessary to explain plate-tectonics.
- Depth– and temperature–dependence of all physical parameters
  $\Rightarrow$ compressible models may be necessary.
- Variations of composition at various scales.
- Two–phase flow (not covered).

Outline

Earth heat budget (Jaupart et al., 2015):

- Total heat flow at the surface of the solid Earth is $\simeq 46\,\mathrm{TW}$.
- Total radiogenic heat production is $\simeq 20\,\mathrm{TW}$.

$\Rightarrow$ Important to consider internal heating.

- And also secular cooling, which is equivalent (Krishnamurti, 1968): Consider that the average temperature $\langle T \rangle$ decreases with time on a long timescale t_a compared to the dynamical one t_c. Time derivative of temperature can be separated in slow and fast contribution so

$$\rho C \left(\frac{\partial T}{\partial t_c} + \vec{u} \cdot \vec{\nabla} T \right) = k \vec{\nabla}^2 T + \underbrace{\rho h - \rho C \frac{\mathrm{d} \langle T \rangle}{\mathrm{d} t_a}}_{\text{effective internal heating}}$$

- With the same choice of scaling, the dimensionless equation is

$$\frac{\partial T}{\partial t} + \vec{u} \cdot \vec{\nabla} T = \vec{\nabla}^2 T + H \text{ with } H = \frac{\rho h d^2}{k \Delta T}$$

- At infinite *Pr*, two dimensionless parameters: *Ra* and H or *Ra* and $Ra_h = Ra H$.

Planform for internally heated convection

- The dynamics is dominated by downwelling cold plumes.
- Hot plumes are often triggered by the spreading of cold matter on the bottom boundary layer.
- Heat transfer is dominated by advection associated with cold currents.

Temperature profiles with internal heating

Sotin and Labrosse (1999)

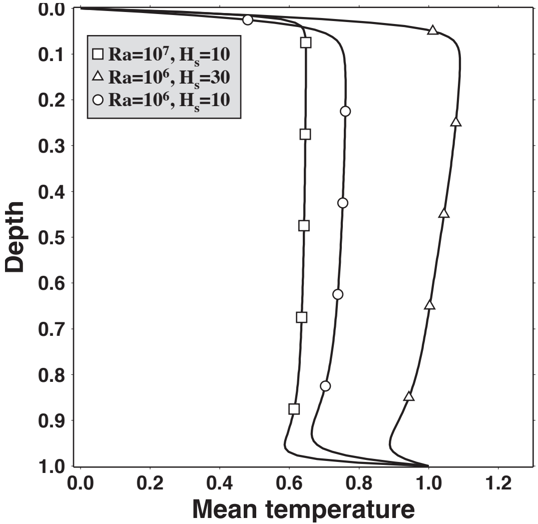

- Two dimensionless parameters *Ra* et H.
- Surface heat flux controlled by the stability of the boundary layer. Local Rayleigh number:

$$\mathit{Ra}_\delta = \frac{\Delta T_s}{\Delta T}\frac{\delta^3}{d^3}\mathit{Ra} = R_c$$

$$\Rightarrow q = \frac{k\Delta T_s}{\delta}$$

$$= \frac{k\Delta T}{d}\left(\frac{\mathit{Ra}}{R_c}\right)^{1/3}\left(\frac{\Delta T_s}{\Delta T}\right)^{4/3}$$

Outline

Toroidal-poloidal decomposition of surface velocity (Ricard & Vigny, 1989)

- Incompressibility $\vec{\nabla} \cdot \vec{u} = 0$

$\Rightarrow$ $\vec{u}$ can be written as

$$\vec{u} = \underbrace{\vec{\nabla} \times T\vec{e}_z}_{Toroidal} + \underbrace{\vec{\nabla} \times \vec{\nabla} \times S\vec{e}_z}_{Poloidal}$$

- For a uniform viscosity, the equation for momentum conservation gives

$$\nabla^4 S = \frac{\delta\rho g}{\eta} \; ; \qquad \nabla^2 T = 0 \Rightarrow \text{no transform fault!}$$

- If η is laterally variable:

$$\eta \nabla^2 \omega_z + \vec{\nabla}\omega_z \cdot \vec{\nabla}\eta = -\frac{1}{\eta}(\vec{\nabla}\eta \times \vec{\nabla}p) \cdot \vec{e}_z$$

$\Rightarrow$ Horizontal gradient of viscosity are necessary to produce toroidal motion.

Surface deformation

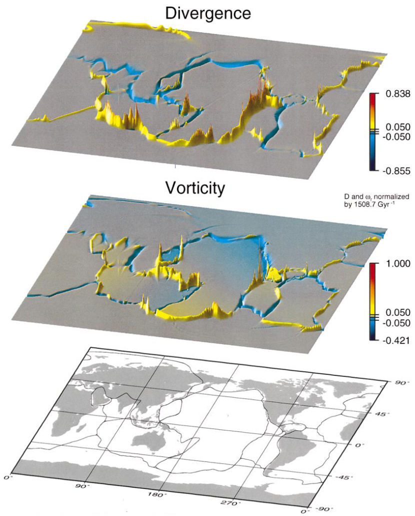

Figure 7. Same as Fig. 6 but with horizontal divergence and radial vorticity calculated directly from the velocity field of the SEISMAR plate model.
(Dumoulin et al, 1998)

(Dumoulin et al., 1998)

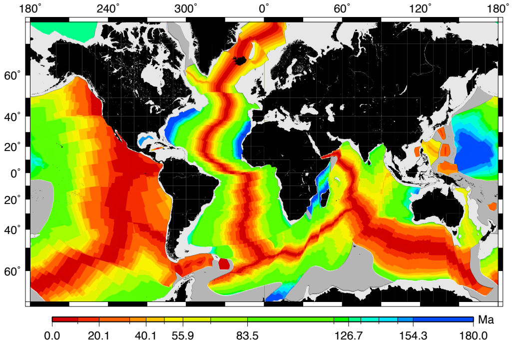

- Seafloor ages
  $\rightarrow$ plate velocities.
- Two types of motion:
  - Convergence (subduction) and divergence (ridges).
  - Strike-slip (Transform faults).

Temperature–dependence of viscosity
White (1988)

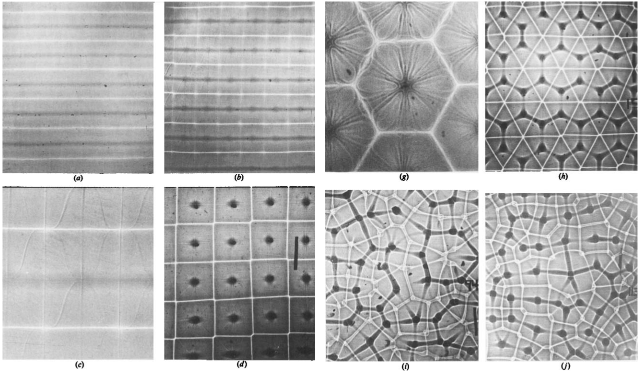

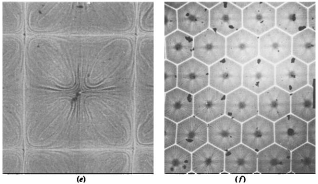

White (1988):
a : rolls
b, c : bimodal
d, e : square
f, g : hexagones
h : triangles
i, j : spoke

- First effect: breaking the symmetry between up- and downwelling currents.

⇒ Allows different flow geometries.

- These experiments: modest variations of viscosity.

Large temperature-dependence of viscosity I

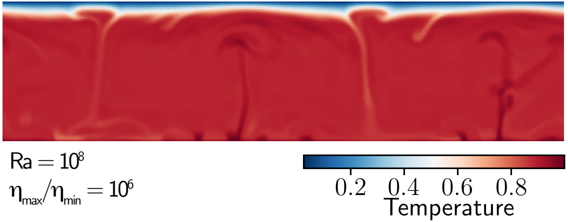

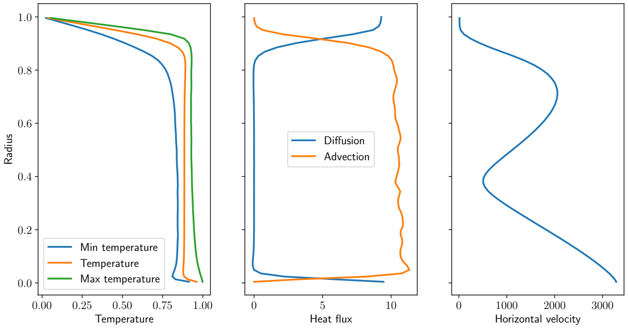

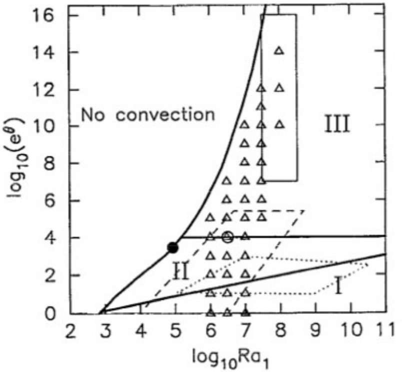

(Moresi and Solomatov, 1995) identified 3 regimes:

- I: small viscosity contrast regime
- II: transitional regime
- III: stagnant lid regime

Strain localisation by pseudo-plasticity
Tackley (2000)

- Temperature dependence of viscosity allows to rigidify plates:

$$\eta(T) = \eta_0 \, e^{E/RT}$$

- A yield stress σ_y is introduced to saturate stress once a critical deformation is reached:

$$\eta_{eff} = \text{min}\left[\eta(T), \frac{\sigma_y}{2\dot{\varepsilon}}\right]$$

with $\dot{\varepsilon} = \sqrt{\dot{\varepsilon}_{ij}\dot{\varepsilon}_{ij}}$

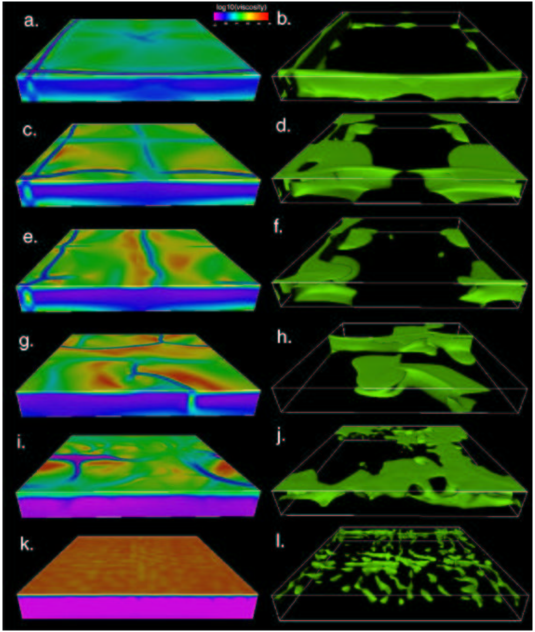

Tackley (2000)

- Left: effective viscosity
- Right: temperature
- Yield stress increases from top to bottom, $34\ \mathrm{MPa}$ to $340\ \mathrm{MPa}$

Heat flow and plate size
Grigné et al. (2005)

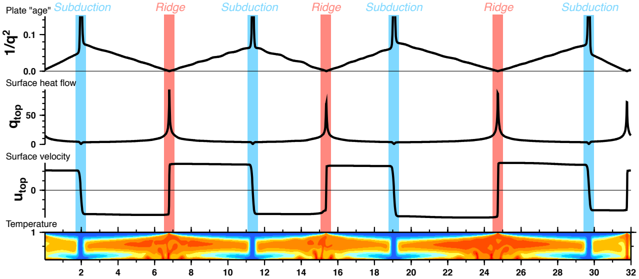

(Grigné et al, 2005 ; Labrosse & Jaupart, 2007)

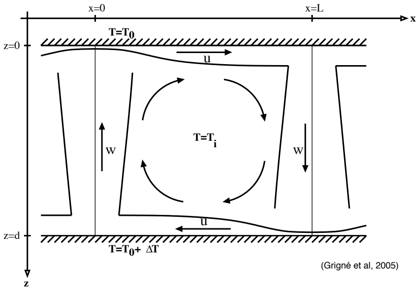

(Grigné et al, 2005)

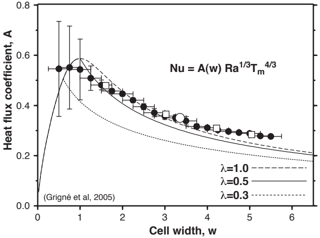

(Grigné et al, 2005)

- Loop model: balance between buoyancy and viscous resistance

$$\Rightarrow q_{top} = C(L) Ra_m^{1/3} T_m^{4/3}$$

$\Rightarrow$ classical scaling supported by convection models with self-consistent plate tectonics (pseudo-plastic rheology).

A rather simple rheology (pseudo-plastic) allows to obtain a dynamics mimicking some aspects of plate tectonics. But...

- How does it relate to the actual rheology of rocks? In particular the yield stress necessary to get plate-like behaviour is generally smaller than that measured in laboratory.
- On Earth, old deformation structures often get reactivated $\rightarrow$ the rheology is history dependent. A damage theory is needed.
  - Bercovici & Ricard (Nature 2014): grain-size dependence in a multi-mineral rock with Zener pinning.
  - Anisotropic viscosity with lattice preferred orientation (Pouilloux et al., 2007)? Theory and models still needed for that.

Outline

- Introduction
- balance equations and the Boussinesq approximation
- Rayleigh-Bénard convection
  - Historical background
  - Linear stability analysis
  - Behaviour beyond the onset
  - High Rayleigh number dynamics and scaling of heat transfer
- Convection in Earth’s mantle
  - Evidences for mantle convection on Earth
  - Internally heated Rayleigh–Bénard convection
  - Temperature–dependence of viscosity and more complex rheologies
  - **Compressibility effects**
  - Variations of composition
    - Models for the present state
    - Evolution models
  - Crust recycling
  - Evolution from a primordial layering

The isentropic temperature gradient

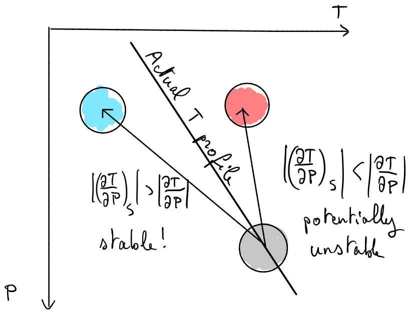

- Compression $\Rightarrow$ increase of temperature $\rightarrow$ useless part of the temperature gradient.
- Isentropic gradient ($\sim$ *adiabatic*)

$$\left(\frac{\partial T}{\partial P}\right)_S = \frac{\alpha T}{\rho C_p} \Rightarrow \frac{\partial T}{\partial r} = -\frac{\alpha g T}{C_p}$$

- Solution to subtract from the total ΔT:

$$T(r) = T_0 \exp\left(-\int_{CMB}^{r} \frac{\alpha g}{C_p}\, dr\right)$$

- T_0 : "foot of the adiabat".
- Jeffreys (1930) showed that the criterion for Rayleigh–Bénard instability in a "weakly compressible" fluid is the same as that derived by Rayleigh (1916) provided the temperature difference is taken as that in excess of the isentropic one.
- Further complexities (i.e. distribution of dissipation) not treated here. See Curbelo, Alboussière et al recent work.

Outline

Compositional variations in the mantle and fluid dynamics

- Upper mantle: direct observations of strong compositional variations from the largest scale (continents and oceans) to the smallest (different minerals in a rock).
- Deep mantle: evidence come from geochemistry and geophysics (mostly seismology).
- Two types of compositional variations:
  - trace elements do not act on density but can play a role on radiogenic heating (^{235}U, ^{238}U, ^{232}Th, ^{40}K).
  - major elements, or oxydes (i.e. FeO and MgO), act on density and most physical parameters, like viscosity.
- In the fluid dynamics of mantle convection: add a new parameter, the buoyancy number

$$B = \frac{\Delta\rho_\chi}{\rho_0\alpha\Delta T} \text{ or } Ra_\chi = Ra B.$$

- The buoyancy term in the momentum equation is:

$$Ra(\theta + BC)$$

  with C the dimensionless composition.

Conceptual models for the current snapshot

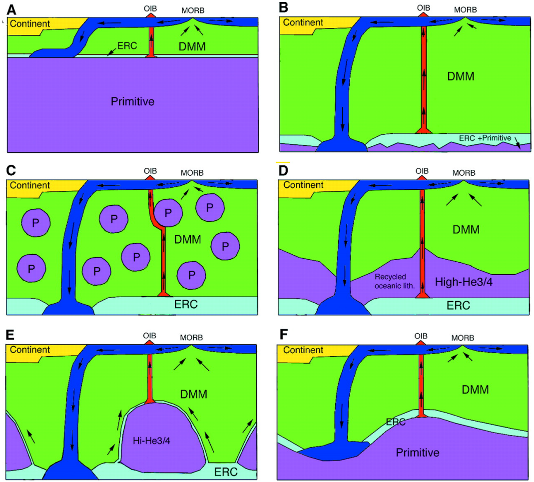

(Tackley, 2000)

Conceptual models for the current snapshot

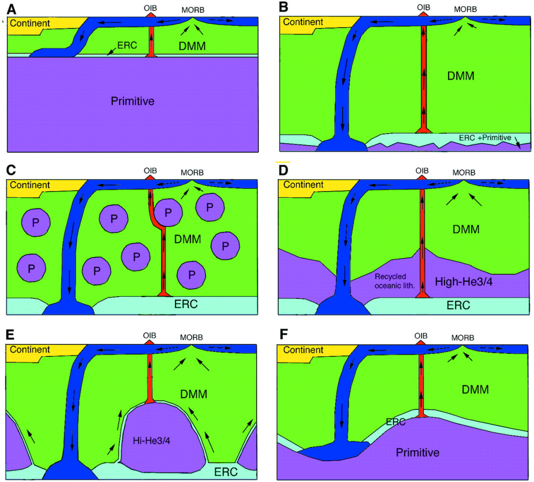

(Tackley, 2000)

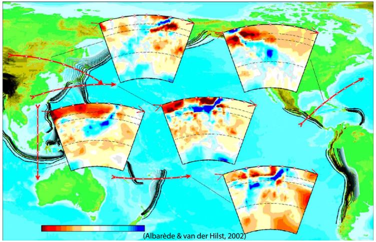

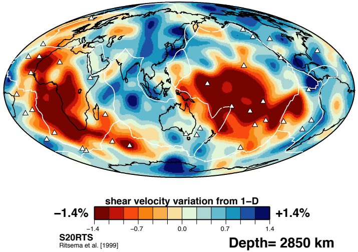

Dense partial melt pocket at the base of the mantle

- Large V_S anomalies in the lower mantle $\rightarrow$ thermal and chemical heterogeneity.
- ULVZs at the edges of dense thermo-chemical piles. Interpreted as pockets of dense partial melt.

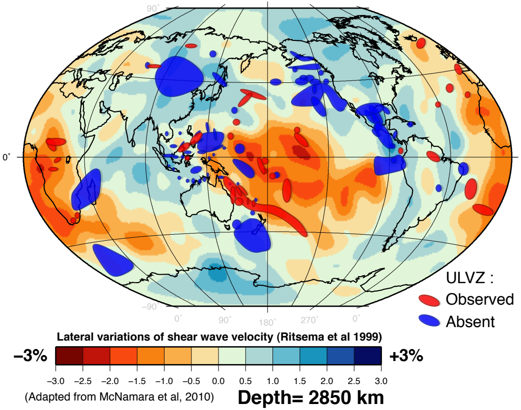

Various observations in Cartoon form
Hernlund & McNamara, ToG 2015

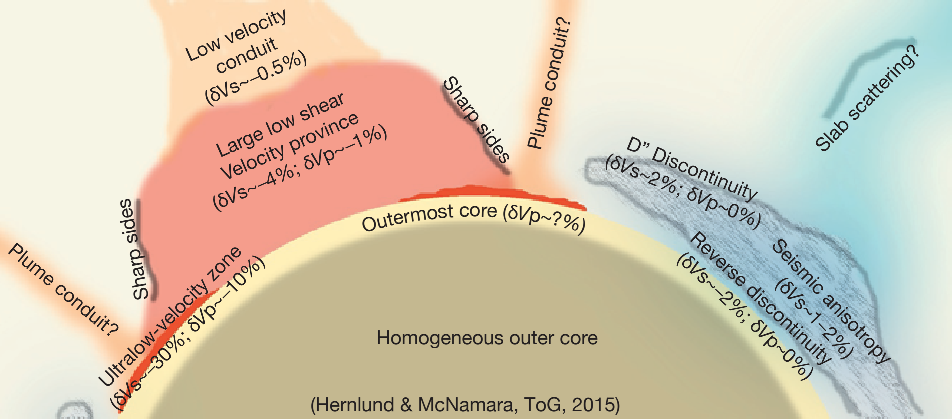

- Also: possible reflection from the top of LLSVPs (Schumacher, et al 2018)
- Simplest common ingredient to all these observations: Compositional variations.

The present snapshot and the long term evolution

- The present observations only constrain the current "snapshot" of the mantle.
- Different timescales of evolution: short (plate tectonics) and long (thermal evolution, regime changes?).
- Avoid the uniformitarian bias!

Stability of LLSVPs?

Burke & Torsvik (2004)

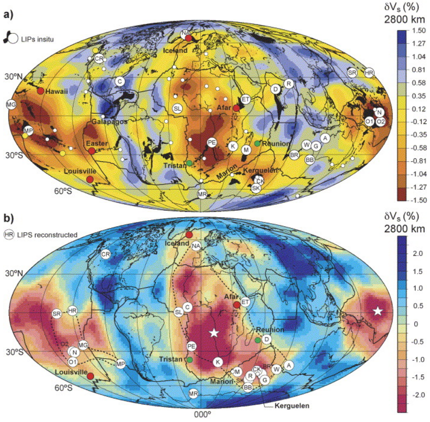

- Position of large igneous provinces (LIPs) when erupted correlates with edges of LLSVPs.
- Suggests "long" (200Ma) term stability of these structures.

LLSVs and ULVZs in models

McNamara, Garnero, Rost (2010)

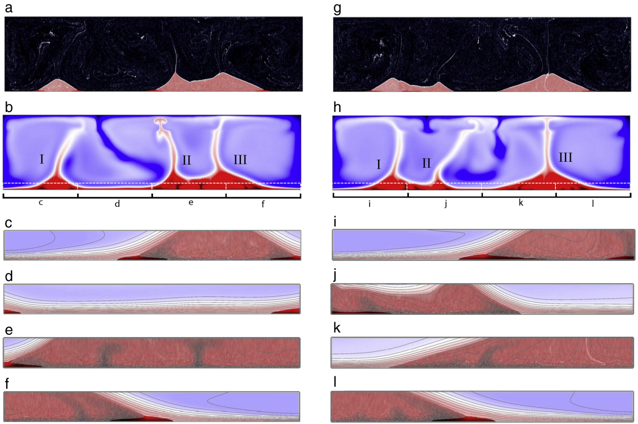

- Dense chemical piles move in response to plate and plume flow.
- ULVZs at the edges.
- But important transient effects.

bridgmanite-enriched ancient mantle structures (BEAMS)

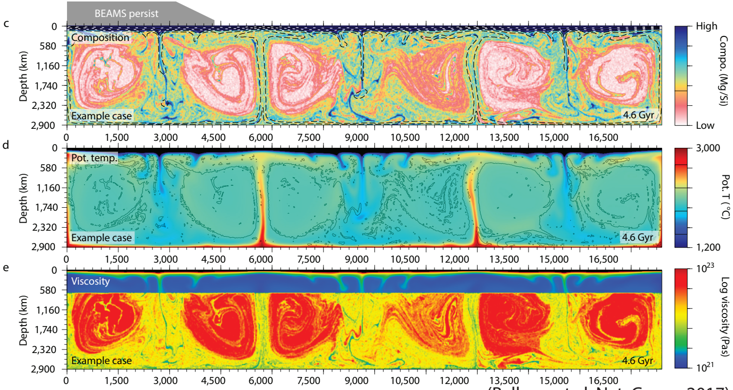

(Ballmer et al, Nat. Geosc. 2017)

- Non-linear viscosity variation depending on Si/Mg ratio.
- For $\eta_{max}/\eta_{min} > 100$ BEAMS forms.

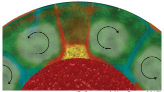

(Ballmer et al, Nat. Geosc. 2017)

- Compositional anomalies are produced at the mineral scale.
- Only a liquid phase permits longer distances separation. This can be
  - water $\rightarrow$ mostly a subduction/mantle corner process, possibly transition zone (Bercovici & Karato, Nature 2003), not covered here.
  - liquid iron $\rightarrow$ often considered limited by the large density contrast. Alternative have been proposed (Kanda & Stevenson, 2006; Otsuka & Karato, 2012) but have not been picked up in geodynamical models.
  - magma $\rightarrow$ fractional melting and freezing creates intermediate ($\sim$ km) scale heterogeneities at the surface (MORB) and possibly in the deep mantle (ULVZ), now and in the past (magma ocean).
- Large scale heterogeneities require entrainment and separation by solid mantle flow.

Outline

Crust recycling

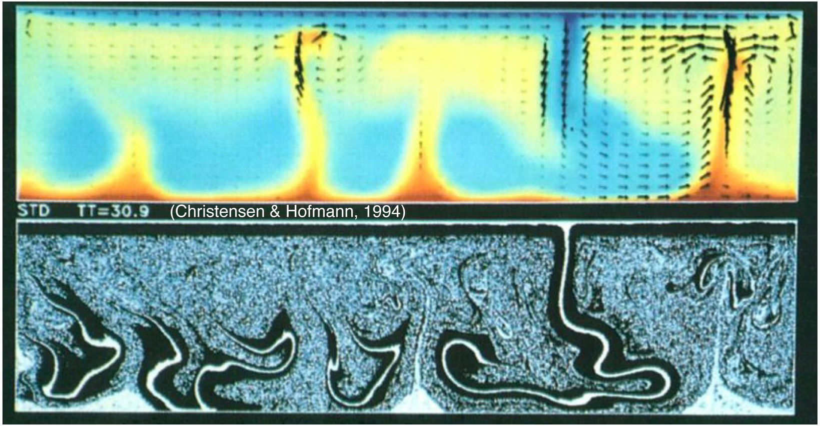

- Partial melting at ridges $\Rightarrow$ production of compositional anomalies.
- Crust minerals become more dense than average mantle at high pressure $\Rightarrow$ it could segregate into the deep mantle.

Effect of numerical resolution

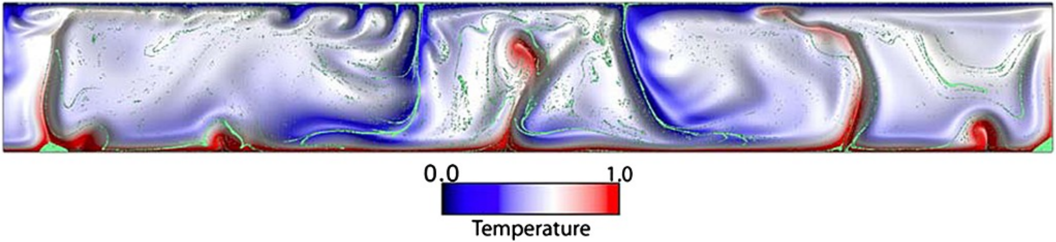

- Most models have a thick crust because of resolution issues.
- High resolution calculations (fig. from Li and McNamara, 2013) show that a 6km thick crust is more difficult to segregate.
- Segregation can be helped by the presence of weak post-perovskite (Nakagawa & Tackley, 2013).
- Also, Wang et al. (2020) show that MORBs at CMB conditions are faster than normal mantle, not slower!

Outline

Entrainment with time
(Le Bars & Davaille, 2004

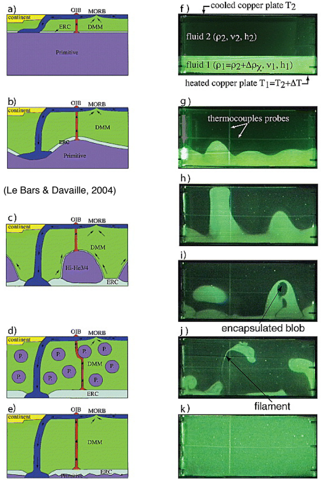

(Le Bars & Davaille, 2004)

- Gradual entrainment at the interface of a layered system makes it undergo regime transitions.
- Doming regime (Davaille, 1999) could explain the anomalous topography of the Pacific superswell and south Africa.
- An intrinsically denser material can become temporally less dense because of high temperature and rise $\Rightarrow$ compatible with LLSVPs less dense than normal mantle (Koeleimejer et al, 2017).
- What could be the origin of the initial layering?

Crystallisation of a basal magma ocean (BMO)
Labrosse et al. (2007)

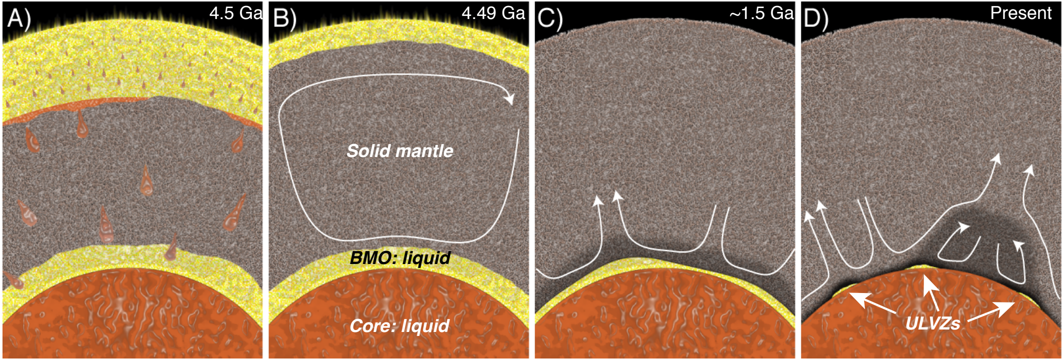

(Labrosse, Hernlund, Coltice, 2007)

- ULVZ: Dense partial melt at present
- Cooling of the core evidenced by the maintenance of the geodynamo for at least 3.5 Gyrs.
- $\Rightarrow$ More melt in the past!
- Fractional crystallisation $\Rightarrow$ compositional variations.

Example of evolution

- Change of dynamical regime with time.
- Gradual stabilisation of a dense layer at the bottom.
- Heat producing elements (HPEs) get to the solid only at the very end of crystallisation $\Rightarrow$ heating up of thermochemical piles that can destabilize.

- Bénard, H. (1900a). Les tourbillons celullaires dans une nappe liquide. Deuxième partie : procédés mécaniques et optiques d'examen. Lois numériques des phénomènes. **12**: 1309–1328.
- Bénard, H. (1900b). Les tourbillons celullaires dans une nappe liquide. Première partie : description générale des phénomènes. **12**: 1261–1271.
- Bénard, H. (1901). Les tourbillons celullaires dans une nappe liquide transportant la chaleur par convection en régime permanent. *Ann. Chim. Phys.* **23**: 62–144.
- Block, M. J. (1956). Surface Tension as the Cause of Bénard Cells and Surface Deformation in a Liquid Film. *Nature* **178**: 650–651.
- Boussinesq, J. (1903). *Théorie Analytique de la Chaleur*. Vol. 2. pp. 157–161. Gauthier-Villars.
- Busse, F. H. (1967). On the stability of two-dimensional convection in a layer heated from below. *J. Math. and Phys.* **46**: 140–149.
- Clarté, T. T., N. Schaeffer, S. Labrosse, and J. Vidal (2021). The effects of Robin boundary condition on thermal convection in a rotating spherical shell. *J. Fluid Mech.* **918**: 1–35.
- Dumoulin, C., D. Bercovici, and P. Wessel (1998). A continuous plate tectonic model using geophysical data to estimate plate-margin widths, with a seismicity-based example. *Geophys. J. Int.* **133**: 379–389.

- Grigné, C., S. Labrosse, and P. J. Tackley (2005). Convective heat transfer as a function of wavelength: Implications for the cooling of the Earth. *J. Geophys. Res.* **110**: doi:10.1029/2004JB003376, B03409.
- Grigné, C., S. Labrosse, and P. J. Tackley (2007a). Convection under a lid of finite conductivity in wide aspect ratio models: effect of continents on the wavelength of mantle flow. *J. Geophys. Res.* **112**: B08403.
- Grigné, C., S. Labrosse, and P. J. Tackley (2007b). Convection under a lid of finite conductivity: Heat flux scaling and application to continents. *J. Geophys. Res.* **112**: B08402.
- Jaupart, C., S. Labrosse, F. Lucazeau, and J.-C. Mareschal (2015). "7.06 - Temperatures, Heat, and Energy in the Mantle of the Earth". *Treatise on Geophysics (Second Edition)*. Ed. by G. Schubert. Second Edition. Oxford: Elsevier, 223–270.
- Jeffreys, H. (1930). The instability of a compressible fluid heated below. *Math. Proc. Camb. Phil. Soc.* **26**: 170–172.
- Krishnamurti, R. (1968). Finite Amplitude Convection With Changing Mean Temperature. Part 1. Theory. *J. Fluid Mech.* **33**: 445–455.
- Labrosse, S., J. W. Hernlund, and N. Coltice (2007). A Crystallizing Dense Magma Ocean at the Base of Earth's Mantle. *Nature* **450**: 866–869.
- Lister, C. R. B., J. G. Sclater, E. E. Davis, H. Villinger, and S. Nagihara (1990). Heat flow maintained in ocean basins of great age: investigations in the north-equatorial West Pacific. *GJI* **102**: 603–628.

- Moresi, L. N. and V. S. Solomatov (1995). Numerical investigation of 2D convection with extremely large viscosity variations. *Phys. Fluids* **7**: 2154–2162.
- Niemela, J. J., L. Skrbek, K. R. Sreenivasan, and R. J. Donnelly (2000). Turbulent convection at very high Rayleigh numbers. *Nature* **404**: 837–841.
- Oberbeck, A. (1879). Über die Wärmeleitung des Flüssigkeiten bei Berücksichtigung des Strömungen infolge von Temperaturdifferenzen. *Ann. Phys. Chem.* **7**: 271–292.
- Pearson (1958). On convection cells induced by surface tension. *J. Fluid Mech.* **4**: 489–500.
- Pouilloux, L., E. Kaminski, and S. Labrosse (2007). Anisotropic rheology of a cubic medium and implications for geological materials. *Geophysical Journal International* **170**: 876–885.
- Rayleigh, L. (1916). On convection currents in a horizontal layer of fluid, when the higher temperature is on the under side. *Phil. Mag.* **32**: 529–546.
- Ricard, Y., M. Richards, C. Lithgow-Bertelloni, and Y. LeStunff (1993). A Geodynamic Model Of Mantle Density Heterogeneity. *J. Geophys. Res.* **98**: 21895–21909.
- Ritsema, J., H. J. v. Heijst, and J. H. Woodhouse (1999). Complex Shear Wave Velocity Structure Imaged Beneath Africa and Iceland. *Science* **286**: 1925–1928. eprint: `http://www.sciencemag.org/cgi/reprint/286/5446/1925.pdf`.

References IV

- Schlüter, A., D. Lortz, and F. Busse (1965). On the Stability of Steady Finite Amplitude Convection. *J. Fluid Mech.* **23**: 129–144.
- Smith, W. H. F. and D. T. Sandwell (1997). Global Sea Floor Topography from Satellite Altimetry and Ship Depth Soundings. *Science* **277**: 1956–1962. eprint: `http://science.sciencemag.org/content/277/5334/1956.full.pdf`.
- Sotin, C. and S. Labrosse (1999). Three-dimensional Thermal convection of an isoviscous, infinite–Prandtl–number fluid heated from within and from below: applications to heat transfer in planetary mantles. *Phys. Earth Planet. Inter.* **112**: 171–190.
- Tackley, P. J. (2000). Self-Consistent Generation of Tectonic Plates in Time-Dependent, Three-Dimensional Mantle Convection Simulations 1. Pseudoplastic yielding. *Geochem. Geophys. Geosyst.* **1**: 2000Gc000041.
- Wang, W., Y. Xu, D. Sun, S. Ni, R. Wentzcovitch, and Z. Wu (2020). Velocity and density characteristics of subducted oceanic crust and the origin of lower-mantle heterogeneities. *Nature Communications* **11**: 1–8.
- White, D. B. (1988). The Planforms And Onset Of Convection With A Temperature-Dependent Viscosity. *J. Fluid Mech.* **191**: 247–286.

Bonus

- Integrate the energy balance equation between the top boundary and any depth z, averaged over time:

$$q_{top} \equiv -\frac{\partial \overline{T}}{\partial z}\left(z = \frac{1}{2}\right) = -\frac{\partial \overline{T}}{\partial z}(z) + \overline{u_z(T(z) - \overline{T})}.$$

- Increase of velocity with *Ra* makes the advection increase $\Rightarrow$ thickness of boundary layers decreases to match the heat flow.

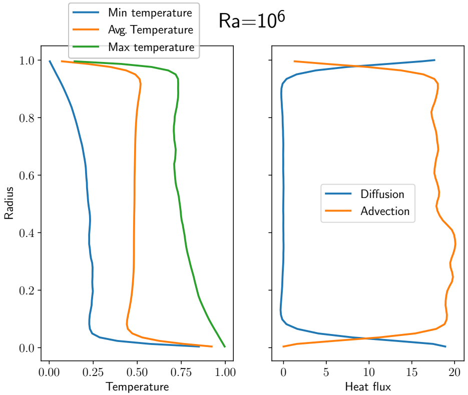

Balance between conduction at the surface and advection at depth

- Heat balance between the surface and depth z :

$$q_0 \equiv \left(k\frac{\partial T}{\partial z}\right)_0 = \underbrace{k\left(\frac{\partial T}{\partial z}\right)_z}_{Conduction} + \underbrace{\rho C_p \overline{w\delta T}}_{Advection} + \underbrace{\rho H z}_{Radioactivity}$$

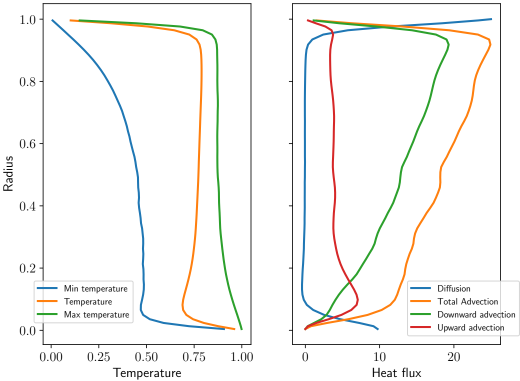

Average temperature
Sotin and Labrosse (1999)

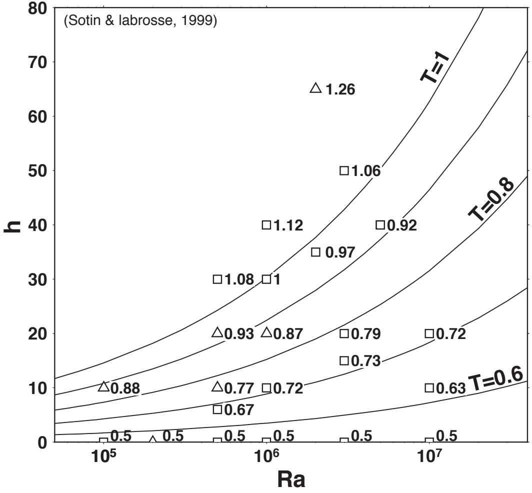

Two contributions:

- Symmetrical case (no internal heating).
- Additional term from internal heating. Total:

$$\frac{\Delta T_s}{\Delta T} = \frac{1}{2} + \frac{H^{3/4}}{Ra^{1/4}}$$